AUV-based observations of small-scale mixing in coastal fronts

Hemantha Wijesekera[1], Timothy Boyd[1], Scott Pegau[1,2], Andrew Dale[1], and Timothy Cowles[1]

[1]College of Oceanic and Atmospheric Sciences, Oregon State University
OC Admin 104, Corvallis, OR 97331

[2]Kachemak Bay Research Reserve, 95 Sterling Hwy, Suite 2
Homer, AK 99603

hemantha@coas.oregonstate.edu
acd@coas.oregonstate.edu
tboyd@coas.oregonstate.edu
tjc@coas.oregonstate.edu
imacc@coas.oregonstate.edu
scott_pegau@fishgame.state.ak.us

Retrieving AUV during the cruise

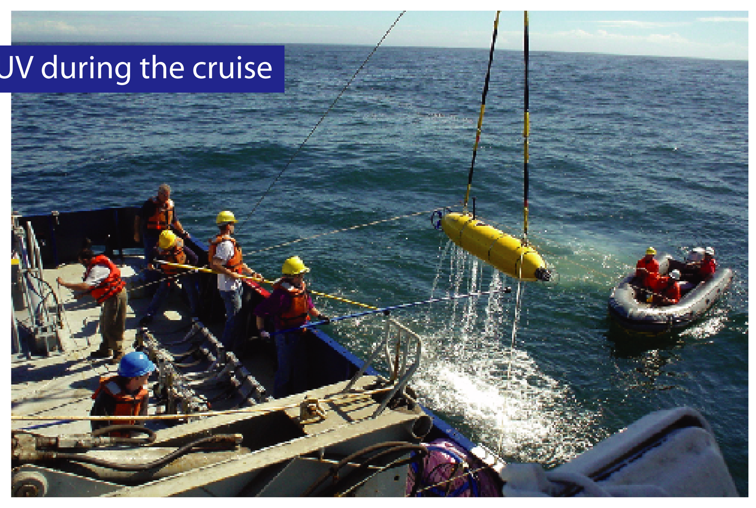

Introduction

Small-scale mixing-processes and bio-optical property distributions over the continental shelf off Oregon were examined from data collected during the summer of 2004. A combination of several different measuring platforms, including an undulating CTD, (Minibat), a free-falling bio-optical profiler, and an autonomous underwater vehicle (AUV) were used to sample the coastal ocean for a period of 10-days from the R/V New Horizon (Figure 1). Simultaneous Minibat-AUV and Profiler-AUV surveys were conducted to acquire biophysical variability over the shallow part of the continental shelf.

Surface winds were weak to moderate, and changed from downwelling favorable direction to upwelling favorable direction during the course of the experiment (Figure 2). During our 10-day stay off the Oregon coast, we captured the upper ocean response to a reversing wind event. We observed strong mixing events caused by non-liner internal waves appearing every semi-diurnal tidal period, and the evolution of biologically active thin layers. Here we discuss small-scale mixing observations across frontal boundaries, while in a companion poster we discuss findings of bio-optical variability over the shelf.

Survey Patterns

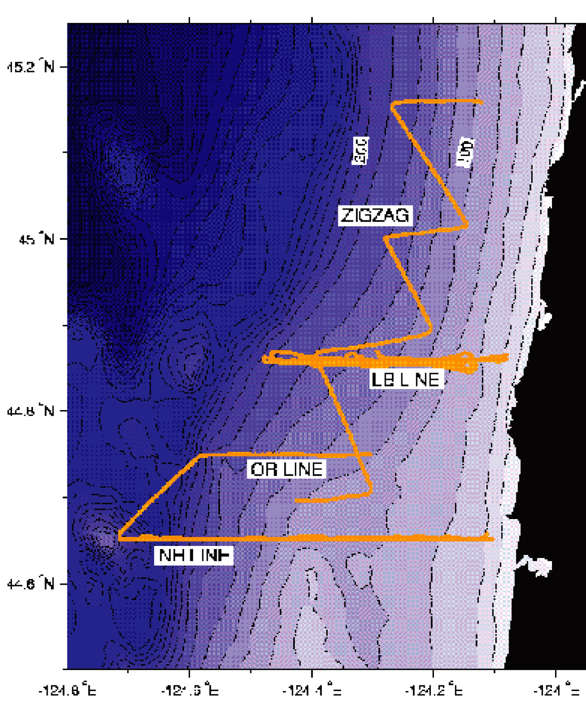

Figure 1. A topographic map showing the experimental site off the coast of Oregon, USA. Thick lines show a composite of Minibat survey paths. AUV operations were limited to the Lincoln Beach Line (LB Line, 44.85N).

Background Meteorology

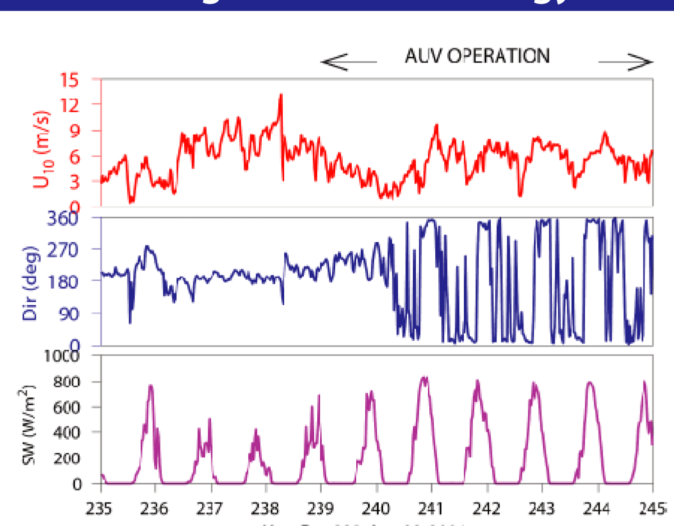

Figure 2. Meteorological variables measured from R/V New Horizon mounted sensor packages: Wind speed U_{10} (top panel), wind direction (middle panel), shortwave radiation SW (bottom panel).

Background Hydrography from MiniBat Surveys

Sequential sections of mesoscale hydrographic fields off Lincoln Beach illustrate Sequential sections of mesoscale hydrographic fields off Lincoln Beach illustrate the temporal and spatial variability of a biological front on the inshore side, a low-salinity warm water (Colombia River plume water) front on the offshore side and thin-biological layers beneath the strongly stratified plume water.

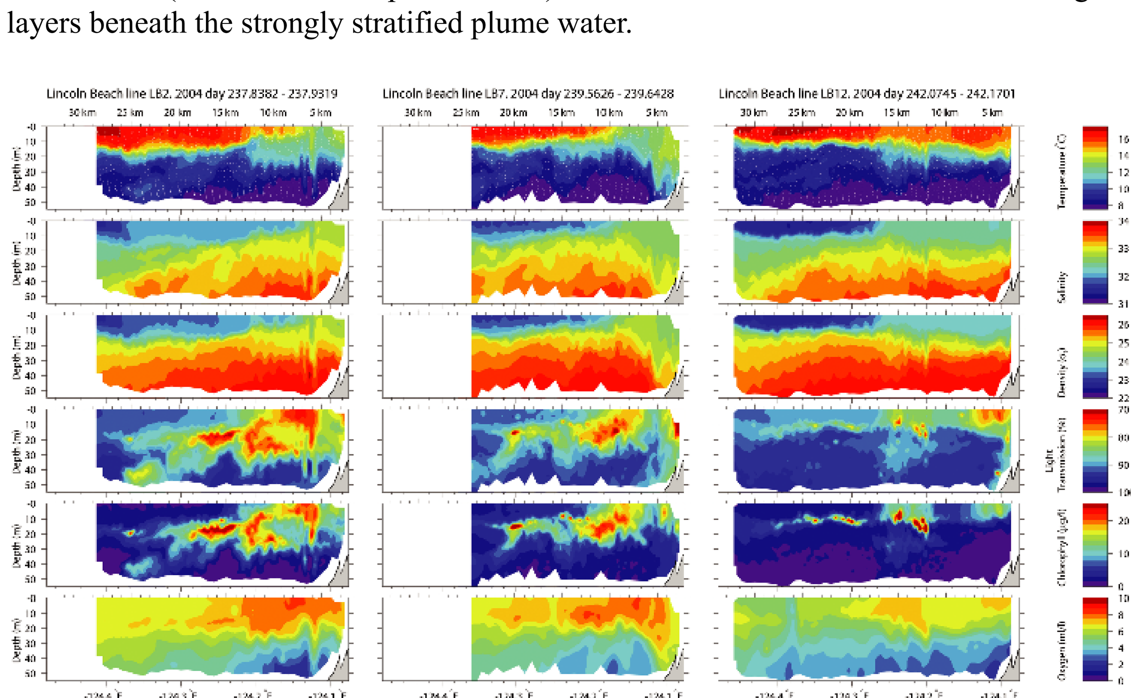

*Figure 3. Depth-longitude plots (top to bottom) of temperature, salinity, density (σ_t), light transmission, chlorophyll, and Oxygen from MiniBat surveys. **Left panel:** survey conducted during Day 237, when winds were downwelling favorable with magnitude of about 10 m/s (Figure 2). Fine-scale fluctuations indicate a passage of internal solitary waves at x=6km. **Middle panel:** survey conducted during Day 239, when winds were weak ~3 m/s, and start to rotate toward southward. Biological front and downwelling isotherms can be seen on the inshore side of the density front. The surface signature of the biological front can be seen in the photo shown in Figure 4. **Right panel:** survey conducted during Day 242, when winds were upwelling favorable with magnitude of about 6 m/s. The surface signature of the biological front was diminishing, while thin biological layers appeared underneath the plume water. The passage of internal waves have tendency to destroy these layers.*

Figure 4. A picture of the biological front when AUV was crossing the boundary (see also Figure 6), which was approximately nine hours after the Minibat survey shown in the mid panel of Figure 3.

AUV Frontal Surveys

The Bluefin Odyssey III AUV was equipped with SBE25-CTD, upward-looking 1200 kHz RDI ADCP and downward-looking 300 kHz RDI DVL/ADCP, a microstructure package (micro-scale conductivity sensor, fine-scale FP10 temperature sensor, two shear probes, pressure sensor, three-axis linear accelerometer, turbidity sensor), an ISUS nitrate sensor, an AC9 - nine-channel optical spectrometer, an optical scattering sensor, and an upward looking 7-channel irradiance sensor (Figure 5). Typical operating speeds of the AUV vary between 3 and 4 knots.

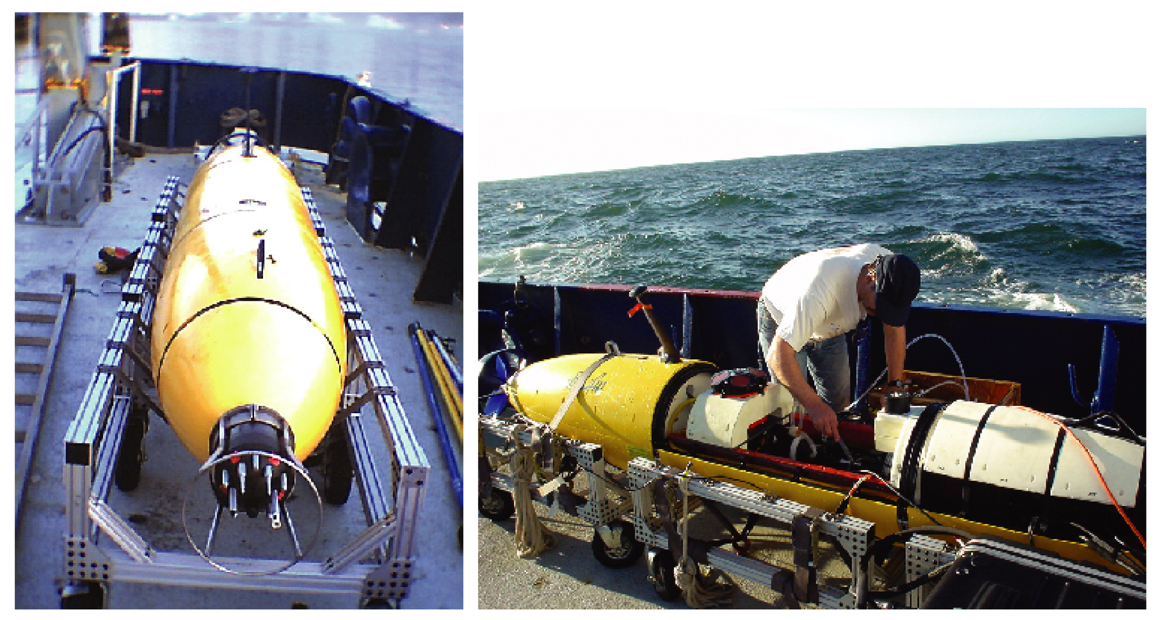

Figure 5. AUV payload: the microstructure package is at the nose and the CTD (not shown) is mounted just below microstructure package (left panel); opened payload section shows the irradiance sensor and the 1200 kHz ADCP at the top. Scott Pegau servicing the AC-9. All the optical sensors are in the mid-payload section. AUV navigational and control servos are in the tail cone section while batteries are in the front section.

After identifying frontal features in real-time MiniBat data, we deployed the AUV to measure small-scale to sub-mesocale variability associated with the features of interest. Detailed observations of a biological/plume frontal boundary are shown in Figure 6. We captured the frontal structure during the passage of internal solitary waves, during which mixing was intense at the frontal boundary.

Solitary Waves at the Plume/Biological Frontal Boundary

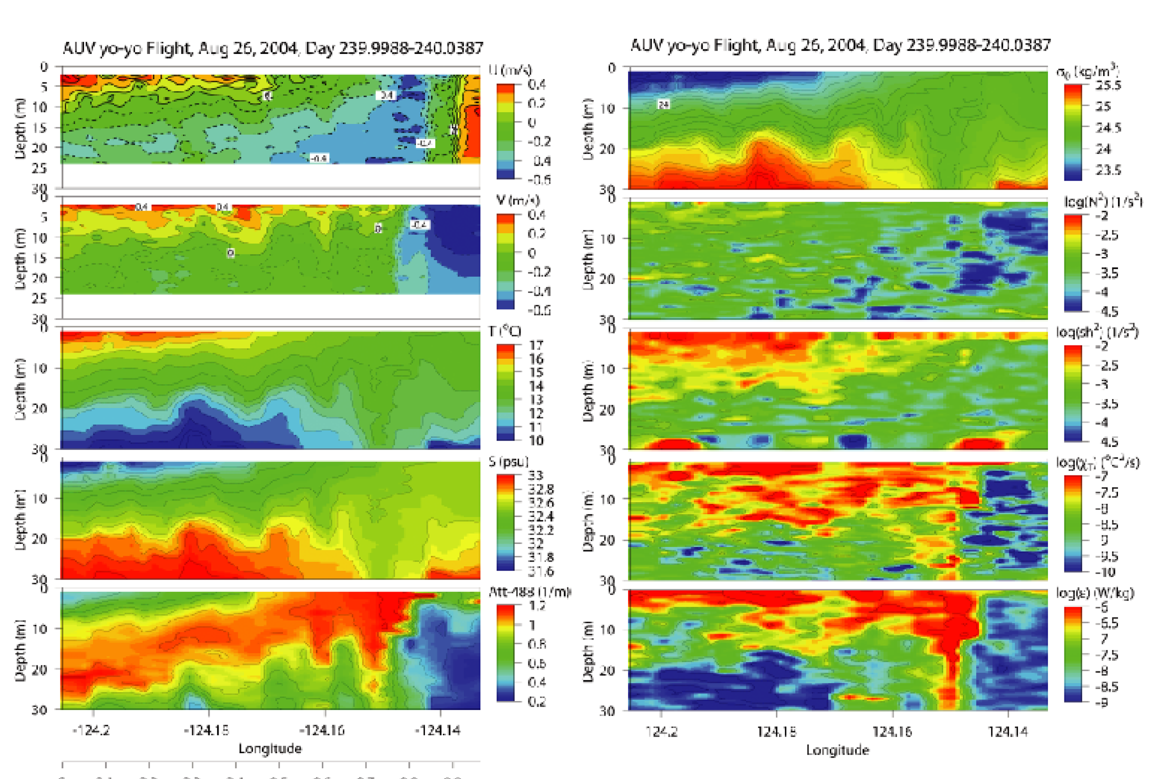

*Figure 6. Depth-longitude fields from an AUV saw-tooth ("yo-yo") mission. **Left panel** (from top to bottom): horizontal currents (U, V) from the upward looking 1200 kHz ADCP; temperature and salinity from the CTD, light attenuation at 488 nm wavelength (Att-488 or c(488)) from the AC-9. **Right panel:** σ_t, buoyancy frequency squared (N^2), shear squared (sh^2), turbulence temperature variance dissipation rate (χ^T), and turbulent kinetic energy dissipation rate (ε). 1-m scale vertical shear was estimated from 15-sec and 1-m vertical meter averaged U and V. The typical operational speed of AUV was about 1.8 m/s. AUV measurements were made during a passage of solitary wave train at the frontal boundary.*

Solitary Waves and Turbulent Mixing

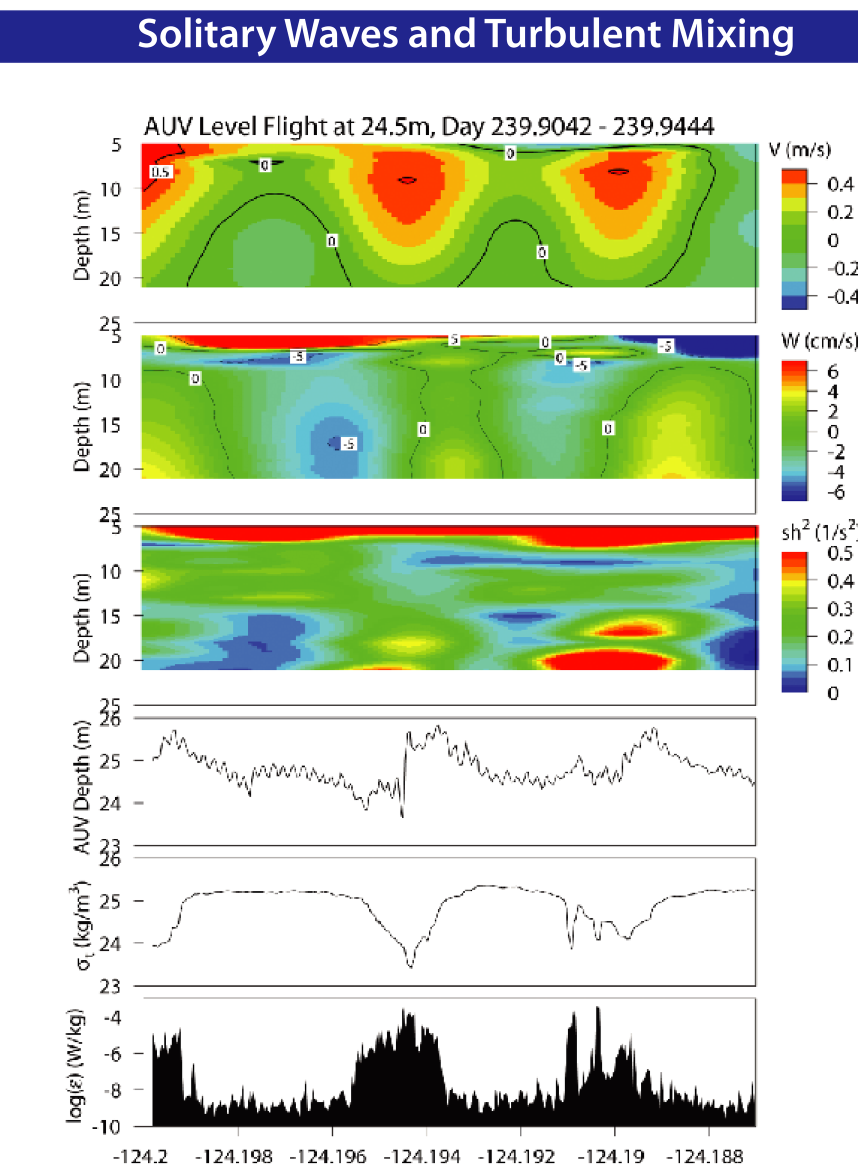

Figure 7. Some detailed measurements of the solitary wave train, collected nearly 2.2 hours prior to the AUV frontal crossing shown in Figure 6. These measurements were made while the AUV was conducting a level flight at a depth of 24.5 m. From top to bottom: 15-sec averaged North-South velocity (V), vertical velocity (W), squared shear (sh^2) from 1200 kHz ADCP, AUV depth, density, and TKE dissipation rate along the AUV path. TKE dissipation rate increased by a factor of about 1000 during the passage of the internal solitary waves.

Cruise-Averaged Mixing Rates

Averaged profiles of temperature, salinity, and σ_t TKE dissipation <ε>, rate, eddy diffusivity, $K_\rho = \langle 0.2\varepsilon/N^2 \rangle$ are shown in Figure 8. The eddy diffusivity in the upper 30 m was ~10^{-4} m^2/s, which was dominated by mixing associated with solitary wave packets.

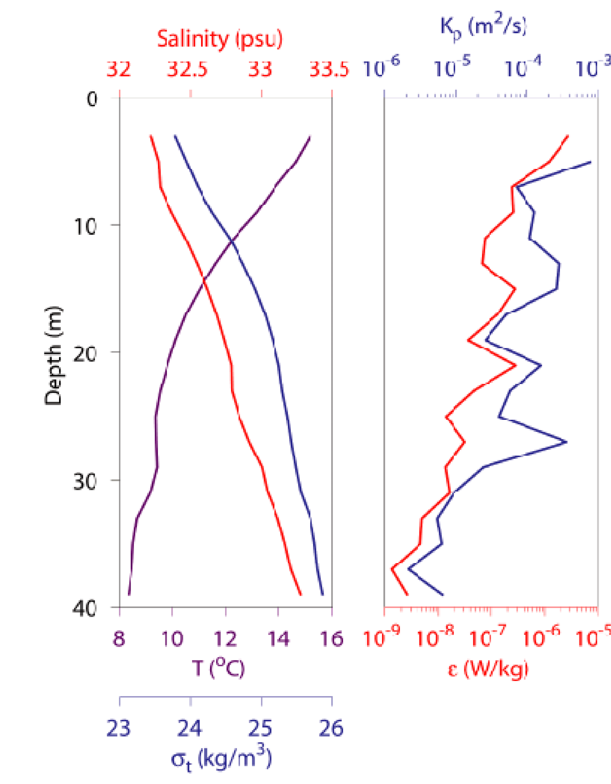

Figure 8. Cruise-averaged profiles of temperature, salinity, and σ_t (left panel) and TKE dissipation rate and eddy diffusivity (right panel) over the mid-shelf off Lincoln Beach.

Scaling TKE Dissipation Rate

Consider the steady state TKE equation in a simple form (neglecting advection, pressure-velocity correlations, and divergence terms)

$$\overline{u'w'}\frac{dU}{dz} = B - \varepsilon \tag{1}$$

where $\overline{u'w'}$ is the turbulence momentum flux, U is the mean flow speed, B is the buoyancy flux, and ε is the TKE dissipation rate. We write turbulent momentum flux as a down-gradient flux term: $\overline{u'w'} = -K_m \frac{dU}{dz}$, where K_m is the eddy viscosity.

Suppose eddy viscosity is a function of Richardson Number Ri,

$K_m \approx C\, Ri^{-n} \approx C\left[\frac{dU}{dz}\right]^{2n} N^{-2n}$, where C and n are constants, and N is the buoyancy frequency. For shear-driven turbulence $B \le 0.2\varepsilon$, therefore the TKE dissipation rate is order magnitude same as the shear production term. Therefore, we can scale the TKE dissipation rate as

$$\varepsilon \approx C\left[\frac{dU}{dz}\right]^{2n+2} N^{-2n} \tag{2}$$

- For n = 1, we recover the *Gregg* [1989] scaling for ε: i.e.,

$$\varepsilon \approx C\left[\frac{dU}{dz}\right]^{4} N^{-2} \tag{3}$$

which yields eddy viscosity $K_m \approx C\, Ri^{-1}$, and eddy diffusivity $K_\rho \approx 0.2C\, Ri^{-2}$;

- For n = 1/2, we can obtain $\varepsilon \approx C\left[\frac{dU}{dz}\right]^{3} N^{-1}$. (4)

which yields $K_m \approx C\, Ri^{-1/2}$ and $K_\rho \approx 0.2C\, Ri^{-3/2}$. The Ri dependencies of the n=1/2 diffusivities are similar to those suggested by *Munk and Anderson* [1948].

Functional forms of the dissipation rate for n = 1 [*Gregg*, 1989] (equation 3), and for n = 1/2 [*Munk and Anderson*,1948] (equation 4) are given in Figure 9A.

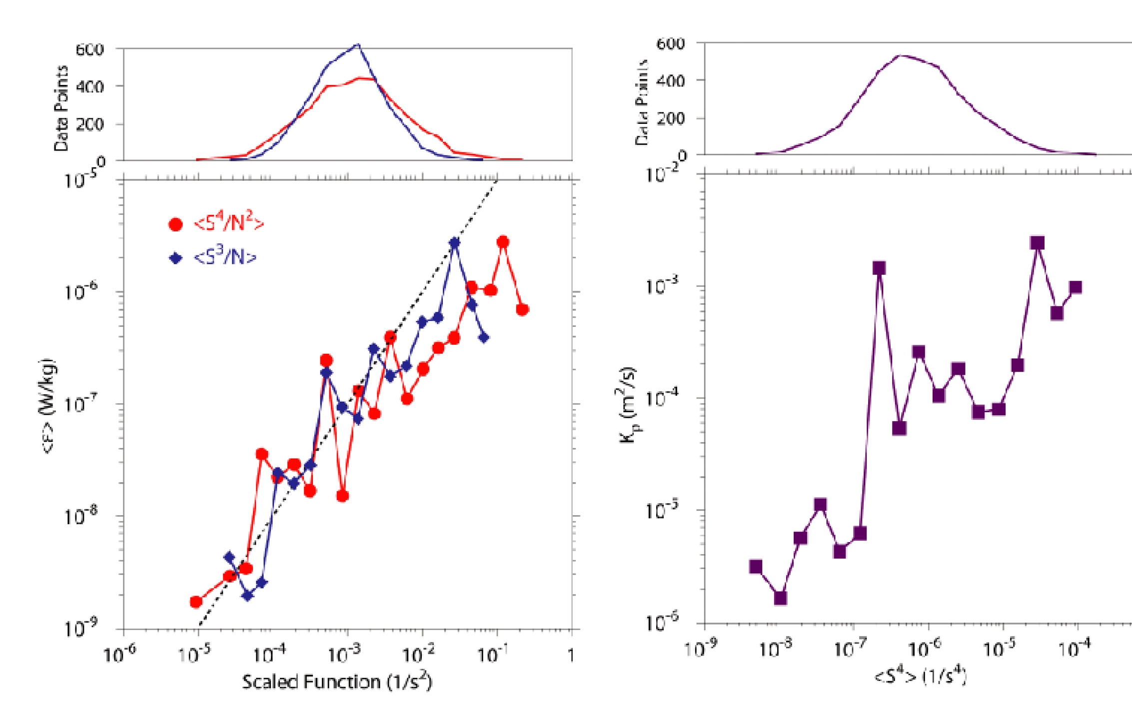

*Figure 9. **Left panel (A):** Scaling given in equation (2): for n=1 $\langle S^4/N^2\rangle$ vs <ε> (red line with bullets), and for n=1/2 $\langle S^3/N\rangle$ vs <ε> (blue line with solid squares), where S is the 1-m scale total shear magnitude. The angle brackets denote cruise average. Top panel shows number of data points averaged in $\langle S^4/N^2\rangle$ (red) and $\langle S^3/N\rangle$ (blue) bins. Dashed line denotes +1 slope. C is about 10^{-4} m^2/s. **Right panel (B):** Cruise-averaged fourth moment of 1-m scale shear $\langle S^4\rangle$ vs eddy diffusivity K_ρ, which is defined as $0.2\varepsilon/N^2$. Top panel shows number data points averaged in S^4 bins.*

Summary

We conducted a 10-day AUV/MiniBat/BioOptical Profiler survey over the Oregon continental shelf in August 2004. We made AUV measurements concurrently with MiniBat, and Profiler surveys. We identified frontal features in MiniBat transect data, and then deployed the AUV to resolve detailed sub-meso-scale to small-scale structure at the frontal boundary. Some of our findings are summarized below.

- Enhanced turbulent mixing was observed at coastal fronts during passages of internal solitary wave packets. Eddy diffusivity was about 10^{-3}–10^{-4} m^2/s during those events. Spatially and temporally averaged eddy diffusivity in the upper 30 m was about 10^{-4} m^2/s.
- TKE dissipation rate was highly correlated with higher order moments of 1-m scale vertical shear of horizontal velocity field.
- Shear-generated TKE dissipation rate can be scaled as

$$\varepsilon \approx C\left[\frac{dU}{dz}\right]^{2n+2} N^{-2n} \quad \text{with eddy viscosity } K_m \approx C\, Ri^{-n}.$$

We noted that for n = 1, we obtain the Gregg (1989) scaling. The functional form of scaled dissipation rate for n = 1/2 is close to the observed dissipation rate, however the scaled dissipation rates for n = 1 and n = 1/2 are not statistically different for our data set (Figure 9A). The estimated C for both n = 1 and n = 1/2 is about 10^{-4} m^2/s.

References

Gregg, M. C., 1989: Scaling turbulent dissipation in the thermocline, *J. Geophys. Res., 101(C5)*, 12217-12238.

Munk, W. H., E. R. Anderson, 1948: Notes on a theory of the thermocline, *J. Mar. Res., Vol VII, No 3*, 276-295.